Journal of Materials Chemistry B



View Article Online PAPER



Cite this: J Mater Chem B 2017 5, 5019

Received 3rd March 2017, Accepted 29th May 2017

DOI: 10.1039/c7tb00598a

rsc.li/materials-b

POSS-ProDOT crosslinking of PEDOT†

Bin Wei, Jinglin Liu, ‡ Lianggi Ouyang and David C. Martin 🕒 §*ab

Alkoxy-functionalized polythiophenes such as poly(3,4-ethylenedioxythiophene) (PEDOT) and poly(3,4propylenedioxythiophene) (PProDOT) have become promising materials for a variety of applications including bioelectronic devices due to their high conductivity, relatively soft mechanical response, good chemical stability and excellent biocompatibility. However the long-term applications of PEDOT and PProDOT coatings are still limited by their relatively poor electrochemical stability on various inorganic substrates. Here, we report the synthesis of an octa-ProDOT-functionalized polyhedral oligomeric silsesquioxane (POSS) derivative (POSS-ProDOT) and its copolymerization with EDOT to improve the stability of PEDOT coatings. The POSS-ProDOT crosslinker was synthesized via thiol-ene "click" chemistry, and its structure was confirmed by both Nuclear Magnetic Resonance and Fourier Transform Infrared spectroscopies. PEDOT copolymer films were then electrochemically deposited with various concentrations of the crosslinker. The resulting PEDOT-co-POSS-ProDOT copolymer films were characterized by cyclic voltammetry, Electrochemical Impedance Spectroscopy, Ultraviolet-Visible spectroscopy and Scanning Electron Microscopy. The optical, morphological and electrochemical properties of the copolymer films could be systematically tuned with the incorporation of POSS-ProDOT. Significantly enhanced electrochemical stability of the copolymers was observed at intermediate levels of POSS-ProDOT content (3.1 wt%). It is expected that these highly stable PEDOT-co-POSS-ProDOT materials will be excellent candidates for use in bioelectronics devices such as neural electrodes.

1. Introduction

Conjugated polymers have gained much interest in a wide range of bioelectronic applications, such as biosensors, drug delivery, tissue engineering, actuators, and neural interfaces. 1-8 These polymers are particularly attractive for neural interface applications due to their relatively soft mechanical properties, tunable surface morphology, high conductivity and excellent biocompatibility. 9-11 These soft materials usually have a typical Young's modulus on the order of ~ 1 GPa and thus are expected to help reduce the mechanical properties mismatch between hard metal electrodes and soft living tissue. 12,13 In addition, they provide high surface areas that can facilitate ion exchange between the microelectrodes and tissue, therefore building more efficient pathways for abiotic-biotic communication.¹⁴ Because of their good electronic and ionic conductivities,

the impedance is usually significantly reduced and charge storage capacity is substantially improved. Among the currently available conjugated polymers, alkoxy-functionalized polythiophenes such as poly(3,4-ethylenedioxythiophene) (PEDOT) and poly(3,4-propylenedioxythiophene) (PProDOT) have become particularly promising candidates because of their low oxidation potential, relatively high chemical and thermal stability, and high conductivity. 15,16 PEDOT-coated electrodes have been widely studied for use in neural interfaces, and their advantages and improvements over conventional metal electrodes have been reported. 17-19 Though conjugated polymers have many advantages over other materials, these materials are often fragile and may delaminate from the surfaces of metal electrodes. 12 Another concern is their electrochemical and mechanical stability for long-term neural recording or stimulation applications. Loss of device performance such as decreased charge carrying capacity and increased impedance of PEDOT coated neural electrodes under chronic neural recording or stimulation conditions has been reported by different groups. 20,21 Not only do these delaminations potentially decrease the charge transfer performance of the devices, but they could also lead to residual fractions of the film left behind in the tissue. It is therefore of interest to make more electrochemically and mechanically stable PEDOT films to improve their long-term performance and minimize the uncertainties this may pose to biological systems.

^a Materials Science and Engineering, The University of Delaware, Newark, DE, 19716, USA

^b Biomedical Engineering, The University of Delaware, Newark, DE, 19716, USA. E-mail: milty@udel.edu

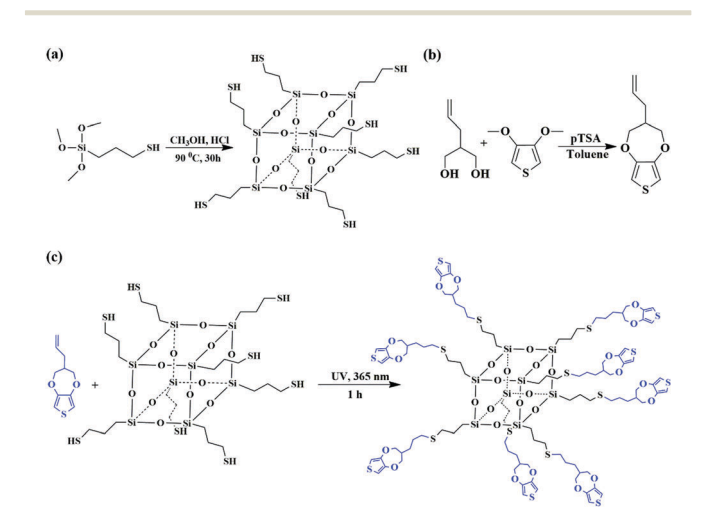
[†] Electronic supplementary information (ESI) available. See DOI: 10.1039/c7tb00598a ‡ Current address: Dow AgroSciences LLC, Indianapolis, IN, 46268, USA.

[§] D. C. M. is a Co-Founder and Chief Scientific Officer for Biotectix LLC, a University of Michigan spin-off company working to develop conjugated polymers for interfacing a variety of electronic biomedical devices with living tissue.

Several strategies have been directed toward improving the electrochemical stability of conjugated polymers on metallic substrates. Cui et al. found that stability of PEDOT films was improved by using carbon nanotubes as dopants during electrochemical polymerization.³ Inganas and coworkers chemically crosslinked the polyelectrolyte dopant PSS and found that the stability of PEDOT:PSS was substantially improved. 22,23 Khodagholy et al. have shown that glycidoxypropyltrimethoxysilane (GOPS) can be used to improve the adhesion and long-term stability of spuncast PEDOT:PSS, while retaining effective charge transport performance.²⁴ The ability to make more mechanically stable PEDOT films by using adhesion promoters has been reported by Wei et al.25 and Carli et al.26

Despite these developments, the search for conducting polymer materials that are more electrochemically and mechanically robust remains an ongoing topic of interest. Recently Ouyang et al. reported the use of a conjugated 3-armed EDOT derivative, 1,3,5-tri[2-(3,4-ethylenedioxythienyl)]-benzene (EPh) as a crosslinker to increase the stability of PEDOT coatings. It was found that the stiffness and fracture resistance were both improved by adding EPh to PEDOT. However the EPh monomer disrupted the conjugation of the chain backbone, leading to dramatic changes in color and a corresponding decrease of the charge transport efficiency. It would therefore be useful to find crosslinking agents for PEDOT that could increase the mechanical performance yet not lead to such a dramatic drop in charge transport properties.

Here, we introduce the use of a ProDOT functionalized polyhedral oligomeric silsesquioxane (POSS) that substantially increases the stability of PEDOT films, while retaining its ability to efficiently transport charge. We took advantage of the cubic POSS cage moiety that consists of 8 silicon atoms at the corners with oxygens along the cube edges (Scheme 1). The POSS core can be chemically functionalized with various organic substituents attached to the silicon corner atoms, forming an organic-inorganic hybrid framework when incorporated into



Scheme 1 Syntheses of POSS-ProDOT crosslinker. (a) Synthesis of POSS-SH via hydrosilylation. (b) Synthesis of ProDOT-ene. (c) Synthesis of POSS-ProDOT via thiol-ene "click" chemistry

other polymer matrices.²⁷⁻²⁹ Functionalized POSS nanomaterials have been previously shown to enhance temperature and oxidation resistance, surface hardening and mechanical integrity of a variety of polymers. For example, the incorporation of POSS units was shown to significantly enhance the electrochemical performance of polyaniline, as shown by cyclic stability testing.27

In this work, we synthesized a functionalized POSS-ProDOT crosslinker via hydrosilylation and thiol-ene "click" chemistry, and subsequently prepared PEDOT-co-POSS-ProDOT copolymers of various compositions by electrochemical polymerization. Since the multifunctional POSS-ProDOT used in this study keeps the reactive thiophene units well away from the center of the crosslinking agent, we anticipated that it would be able to provide the desired increase in electrochemical and mechanical performance without necessarily causing significant disruption in the conjugation of the chains themselves. We expected that the POSS-ProDOT crosslinker would enhance the long-term electrochemical stability of PEDOT coatings while preserving the excellent electrical properties of PEDOT. Our results show that small amounts of POSS-ProDOT (3.1 wt%) do indeed provide substantial improvements in stability without sacrificing toughness or electrical transport performance. However further additions cause the films to become more brittle.

2. Experimental

2.1. Materials

3,4-Dimethoxythiophene, diethyl allylmalonate, lithium aluminum hydride, p-toluene sulfonic acid (p-TSA), tetrabutyl ammonium perchlorate (TBAP), 3-mercaptopropyl trimethoxysilane (MTS), 2,2-dimethoxy-2-phenylacetophenone (DMPA) and 3,4-ethylenedioxythiophene (EDOT) were purchased from Sigma-Aldrich. 2-Allyl-1,3-propanediol was synthesized from diethyl allylmalonate. 15 Stainless steel electrodes (E363/76/SPC) were purchased from Plastics One. ITO coated glass slides were purchased from Delta Technologies with a surface resistivity of 4-8 Ω sq⁻¹. All other chemicals were of analytical grade, and Milli-Q water from a Millipore Q water purification system was used throughout. All reagents and solvents were used without further purification, unless otherwise noted. Samples were irradiated using a UVP Black Ray UV Bench Lamp XX-15L, emitting 365 nm light at 15 W.

2.2. Syntheses of alkene functionalized ProDOT derivative (ProDOT-ene) and POSS-SH

ProDOT-ene was synthesized via the p-TSA catalyzed transetherification route from 3,4-dimethioxythiophene and 2-allyl-1,3propanediol (Scheme 1b) as previously described. 15 H NMR (400 MHZ, CDCl₃): $\delta = 6.48$ (s, 2H); 5.78 (m, 2H); 5.10 (m, 1H); 4.10-4.16 (m, 2H); 3.86-3.92 (m, 2H); 2.18-2.26 (m, 3H).

The synthesis of POSS-SH is shown in Scheme 1a according to literature. 5 mL MTS, 10 mL concentrated hydrochloric acid and 120 mL methanol were added into a 500 mL round bottom flask. The reaction mixture was refluxed at 90 °C for 30 h under

agitation to ensure the completed hydrosilylation. The white viscous precipitate was first washed with methanol for three times and then dissolved in 2 mL THF. The THF solution was added to 100 mL acetonitrile drop wisely and then allowed to crystallize at −20 °C for overnight. The final product was dried in a vacuum oven at room temperature for 12 h, and the yield was 59%. ¹H NMR (600 MHZ, CDCl₃): δ = 2.56 (s, 2H); 1.72 (s, 2H); 1.38 (s, 1H); 0.77 (m, 2H).

2.3. Preparation of POSS-ProDOT via thiol-ene "click" chemistry

POSS-ProDOT was synthesized from POSS-SH and ProDOT-ene. POSS-SH (30 mg, 0.03 mmol) and a minimum of THF were added to a vial and heated to dissolve the thiol. ProDOT-ene (70 mg, 0.35 mmol) and 0.1 wt% of 2,2-dimethoxy-2-phenylacetophenone (DMPA) were added, and the mixture was sparged with argon for five minutes. The vial was placed under a UV lamp and irradiated for one hour (Scheme 1c). A small amount of methanol was added, and the product was ultrasonicated for 2 min. The supernatant was decanted and the product redissolved in chloroform, and concentrated by evaporation to give a viscous oil. The yield of the thiol-ene reaction was 66%. ¹H NMR (600 MHZ, CDCl₃): δ = 6.48 (s, 2H); 4.11 (m, 2H); 3.89 (m, 2H); 2.52 (s, 4H); 2.14 (m, 1H); 1.67 (s, 4H); 1.54 (m, 2H); 0.77 (s, 2H).

2.4. Electrochemical polymerization and characterization

All the electrochemical polymerization and characterization experiments were performed with a Gamry Potentiostatic Reference 600TM in a three electrode cell. Stainless steel electrode (Plastics One) or ITO coated glass (Delta Technologies) served as the working electrode, a platinum plate of 1 cm² surface area was the counter electrode, and Ag/AgNO3 was the reference electrode. The electrochemical characterization of POSS-ProDOT was studied in a dilute (2 mM) dichloromethane solution containing 0.1 M tetrabutyl ammonium perchlorate (TBAP) as supporting electrolyte. PEDOT homopolymer and PEDOT:POSS-ProDOT copolymers with various contents of POSS-ProDOT were prepared under constant voltage (+1.1 V) with a total electrodeposition charge of 27 mC. For CV, the polymer films were scanned between -1.0 V and +0.8 V in a phosphate buffered saline (PBS) buffer solution free of monomer with an Ag/AgCl reference electrode. For EIS, the sample acted as the working electrode, a platinum plate as the counter electrode and PBS as the electrolyte. A sinusoidal AC signal with 10 mV amplitude was applied over a frequency range of 1-10⁵ Hz. Each impedance spectrum was obtained at least three times, and the error bars show standard deviations.

2.5. Characterization

Nuclear Magnetic Resonance (NMR) spectra (¹H, ¹³C and ²⁹Si) were acquired on either a Bruker DRX-400 or Bruker DRX-600 spectrometer. Chemical shifts are reported in parts per million, referenced to chloroform solvent as internal standard (CDCl3: 7.24 ppm for ¹H and 77.2 for ¹³C). Fourier-Transform Infrared (FTIR) spectra were collected on a Perkin Elmer Spectrum 100

spectrometer fitted with a Universal ATR accessory. UV-visible (UV-vis) spectra of the polymer films were collected on a Shimadzu UV-2550 spectrophotometer (Shimadzu, Japan), the polymer films were reduced at -1.0 V for 1 minute before measurement. Scanning Electron Microscopy (SEM) images of the polymer films were acquired using a Zeiss Auriga 60 Focused Ion Beam Scanning Electron Microscope (FIB-SEM) operating at 3 kV.

Results and discussion

3.1. Syntheses and characterization of POSS-SH, ProDOT-ene and POSS-ProDOT

Thiol-functionalized polyhedral oligomeric silsesquioxane (POSS-SH) was synthesized via the direct hydrosilylation of 3-mercaptopropyl trimethoxysilane (MTS) in methanol as shown in Scheme 1a. 30,31 The chemical structure was confirmed by both NMR and FTIR spectra. The thiol functional side groups are critical for the subsequent thiol-ene "click" reaction to make a core material that can act as cross linker during the electrodeposition, thus the existence of the thiol groups needed to be verified first. The ¹H NMR spectrum of POSS-SH with assigned peaks is shown in Fig. 1a. The thiol side group was clearly confirmed by the triplet centered at 1.38 ppm. The presence of the thiol group was also confirmed by an absorption peak located at 2550 cm⁻¹ corresponding to the characteristic absorption of the -SH stretching vibration in FTIR (Fig. S1, ESI[†]). The 3D structure of the POSSbased hybrid material was also confirmed by both NMR and FTIR spectra. The sharp peak located at -67.12 ppm in the ²⁹Si NMR spectrum (Fig. S2, ESI†) indicated that the silicon atoms were all magnetically equivalent, and the T-type silanol silicon peak confirmed that each silicon atom was covalently bonded with three oxygen atoms and one carbon atom. The asymmetric

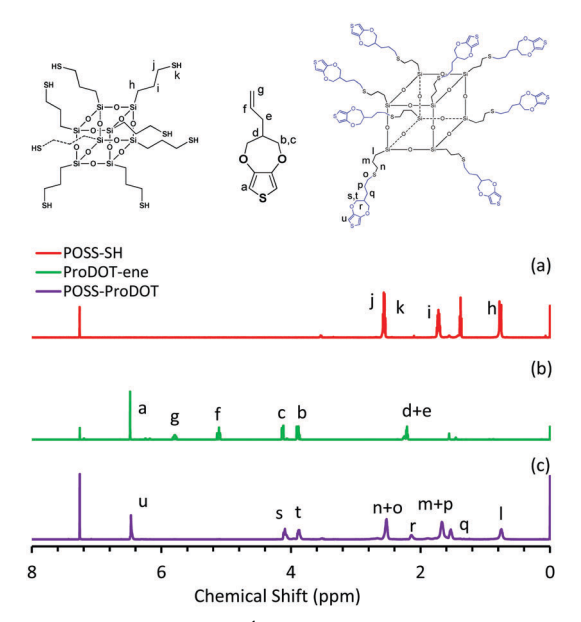


Fig. 1 Chemical structure and ¹H NMR spectra in CDCl3. (a) POSS-SH, (b) ProDOT-ene and (c) POSS-ProDOT.

stretching vibration of Si-O-Si at 1082 cm⁻¹ and 1000 cm⁻¹ in FTIR confirmed the cage-like structure as well (Fig. S1, ESI†). As shown in Scheme 1b, ProDOT-ene was synthesized via p-TSA catalyzed transetherification from 3,4-dimethioxythiophene and 2-allyl-1,3-propanediol. The ProDOT-ene was purified as a light yellow viscous liquid and the chemical structure was confirmed by NMR and FTIR. In Fig. 1b, all the chemical shifts corresponding to each proton on ProDOT-ene are clearly assigned. The two peaks located at 5.2 ppm and 5.8 ppm in ¹H NMR correspond to the protons on the ene moiety. The electroactive cross linker, POSS-ProDOT, was prepared from POSS-SH and ProDOT-ene via thiol-ene "click" chemistry with 0.1 wt% DMPA as radical initiator. 32 As was confirmed by both ¹H NMR (Fig. 1c) and FTIR (Fig. S1, ESI†), the disappearance of the three peaks located at 1.38 ppm, 5.2 ppm and 5.8 ppm in ¹H NMR and changes of the characteristic peaks associated with the alkene group on the ProDOT-ene (=C-H bend at 916 and 994 cm $^{-1}$ and C=C stretch around 1639 cm $^{-1}$) and the -SH group on the POSS-SH (-SH bend at 2550 cm⁻¹) indicated the success of the thiol-ene reaction.

3.2. Electrochemical studies of POSS-ProDOT, EDOT and **EDOT/POSS-ProDOT mixed solutions**

The electrochemical behavior of POSS-ProDOT crosslinker was investigated via cyclic voltammetry (CV) by potentiodynamically scanning the solution between -0.6 V and +1.5 V (vs. Ag/AgNO₃). Cyclic voltammograms from a typical experiment are shown in Fig. 2. An irreversible oxidation corresponding to thiophene ring from the POSS-ProDOT that occurred at +1.20 V was seen in the first anodic scan (red curve). The fact that the oxidation potential of the cross linker was similar to that of EDOT³³ indicated that it would be relatively easy to get POSS-ProDOT incorporated into PEDOT films. In the subsequent scans, unlike the electrochemical

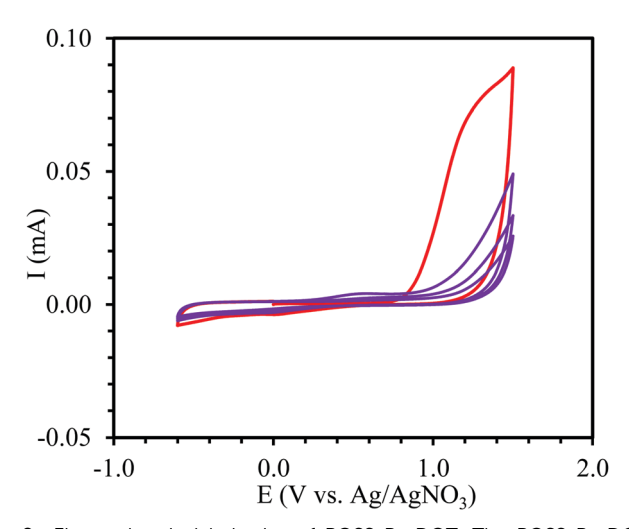


Fig. 2 Electrochemical behavior of POSS-ProDOT. The POSS-ProDOT crosslinker solution (5 mM) was potential dynamically scanned from -0.6 V to +1.4 V in ACN/TBAP (0.1 M) for 4 cycles. An oxidation onset at +1.0 V was observed at the 1st scan (red), no oxidation peaks corresponding to the formation of polymer was observed in the subsequent scans, 2nd to 4th (purple).

polymerization of ProDOT derivatives, no obvious peaks associated with the formation of PProDOT polymers were found at lower potentials during both anodic and cathodic scans. 15 This low polymerizability of POSS-ProDOT is presumably due to the large steric hindrance of the bulky POSS core. It has been reported by several groups that monomers with bulky side groups cannot form their corresponding polymers via direct electrochemical polymerization. 15,34 The electrochemical behaviors of pure EDOT and EDOT/POSS-ProDOT mixed solutions were also studied via cyclic voltammetry and no obvious differences were observed among EDOT and various EDOT/POSS-ProDOT solutions

3.3. Optical properties

PEDOT/POSS-ProDOT copolymer films were obtained by applying a potentiodynamic scan with potential cycling between -0.6 V and +1.2 V (vs. Ag/AgNO₃) for 8 cycles in a series of mixed monomer solutions. The optical properties of the films prepared in mixed monomer solutions didn't change significantly with increasing POSS-ProDOT feed ratio. The electrochemically deposited PEDOT had a blue color due to its partially oxidized state, and the copolymers showed similar colors as the PEDOT thin films. The UV-vis spectra of the polymer films are shown in Fig. S3 (ESI†). All the films were reduced at -1.0 V for 1 minute before measurement and they showed an increasing trend of absorption from 400 to 800 nm, with a local absorption maximum near 600 nm. It was found that the copolymerization shifted the absorption maximum to shorter wavelength. As shown in Table 1, for pure PEDOT thin films, the absorption maximum was 576 nm, while with more and more crosslinker added to the solution, the absorption maximum shifted from 576 nm to 543 nm. The modest 33 nm difference in the absorption maxima also explains the similar blue colors of the pure PEDOT and PEDOT-co-POSS-ProDOT copolymer films. It was previously reported that the absorption maxima of PEDOT films could be significantly tuned by adding a conjugated crosslinker, EPh. Hundreds of nanometers of blue shifts in absorption maxima were observed with EPh as crosslinker, leading to dramatic changes in color.12 The blue shift of absorption was resulted from the decreased conjugated chain length which could potentially lead to an eventual loss in charge transport efficiency, usually larger blue shift could result in more loss of conductivity. However, in this system, much smaller shifts in absorption were observed. These results indicate that the POSS-ProDOT crosslinker does not significantly disrupt the overall conjugation of the PEDOT backbone, making it possible to maintain the desirable electronic properties.35,36

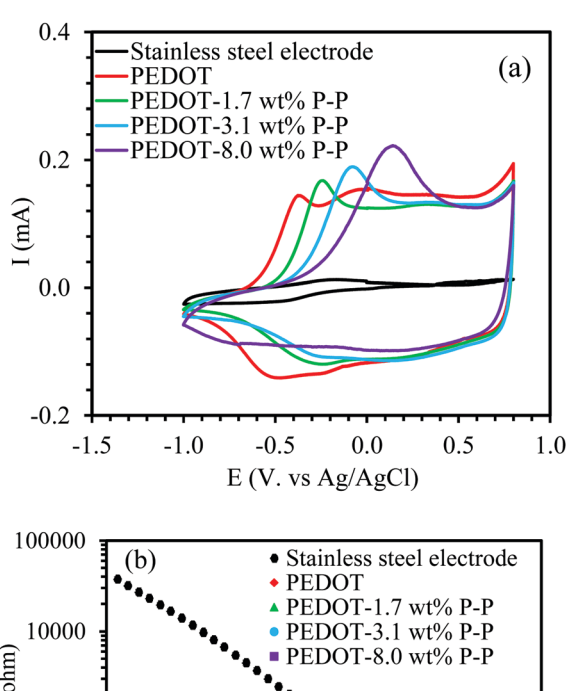
Table 1 UV-vis absorption maxima. The absorption maxima difference of reduced PEDOT and copolymer films indicated that crosslinker does not significantly disrupt the overall conjugation of the PEDOT backbone

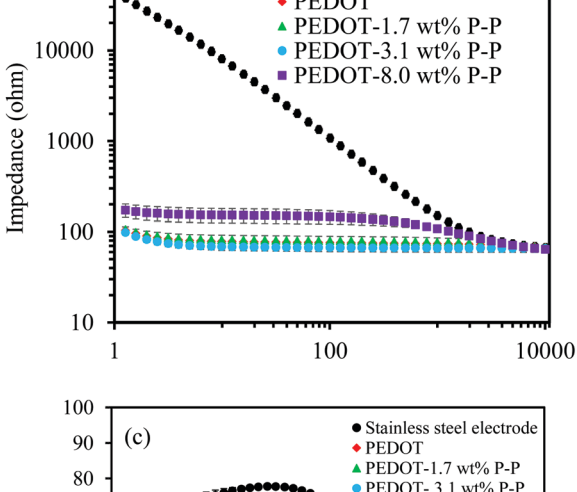
Polymer	Wavelength [nm]
PEDOT	576
PEDOT-1.7 wt% P-P	563
PEDOT-3.1 wt% P-P	549
PEDOT-8.0 wt% P-P	543

3.4. Electrochemical properties

PEDOT and PEDOT-co-POSS-ProDOT copolymers were electrochemically polymerized onto stainless steel electrodes under constant voltage (+1.1 V. a total deposition charge of 27 mC) with tetrabutylammonium perchlorate (TBAP, 0.1 M) as electrolyte in a standard three-electrode cell. We performed both cyclic voltammetry (CV) to determine the charge storage Capacity (CSC) and electrical impedance spectroscopy (EIS) to determine electrode impedance. Cyclic voltammetry of stainless steel electrodes, PEDOT and PEDOT-co-POSS-ProDOT copolymers coated electrodes are shown in Fig. 3a. Both PEDOT and its copolymers showed oxidation and reduction reactions as indicated by the anodic and cathodic current peaks on the CV curve. The peak potential indicates the voltage at which the reaction takes place and the enclosed areas of the curve are proportional to the charge storage capacity. Clearly the PEDOT and the copolymer films have significantly higher charge storage capacities than the uncoated stainless steel electrode. The CV curves of PEDOT and copolymers were of similar shape, while the oxidation peaks shifted to the positive direction with increasing amounts of crosslinker. These shifted oxidation peaks indicated that the crosslinker decreased the conjugation length of PEDOT. 12,35,37

The electrochemical properties of coated electrodes were further investigated using electrical impedance spectroscopy (EIS) in 0.1 M PBS buffer solution. After PEDOT deposition, the amplitude of the impedance of the coated electrodes decreased by 2–3 orders of magnitude (from $\sim 10\,000\,\Omega$ to $\sim 100\,\Omega$) at low frequencies as seen in Fig. 3b. This dramatic drop in impedance has been associated with the increase in effective surface area and ability of the PEDOT to facilitate both electronic and ionic charge transport.38,39 It was also found that at low POSS-ProDOT concentration (<3.1 wt%), the impedance of PEDOT copolymer coated electrodes was similar to the PEDOT-coated electrodes, which were all around 100 Ω . The impedance was slightly increased from 100 Ω to 200 Ω for PEDOT films with higher POSS-ProDOT concentration (8.0 wt%). The increased impedance at higher crosslinker concentration likely comes from three major factors. First of all, POSS nanomaterials are insulating and the excess POSS raises the internal impedance of the PEDOT-8.0 wt% POSS-ProDOT. In addition, the decreased conjugation chain length may be another reason for the increasing impedance. When 1.7% POSS-ProDOT was added, the absorption maximum blue-shifted 13 nm, and a small change in impedance was observed. However, as the feeding ration up to 3.1%, the absorption maximum blue-shifted 27 nm, indicating the conjugation length shortened more significantly, therefore, large variation on impedance can be found. Last but not least, as discussed in more detail in the following section, the crosslinker changed the morphology of the polymer film during the electrochemical deposition as shown in Fig. 4. As increasing the feed ratio of POSS-ProDOT, the morphology of the film became denser, resulting in a higher impedance. It has been reported that films with an open structure usually have lower impedances in comparison to the films with a closed, dense structure. 40 The 8.0 wt% POSS-ProDOT feed ratio had the highest crosslinker





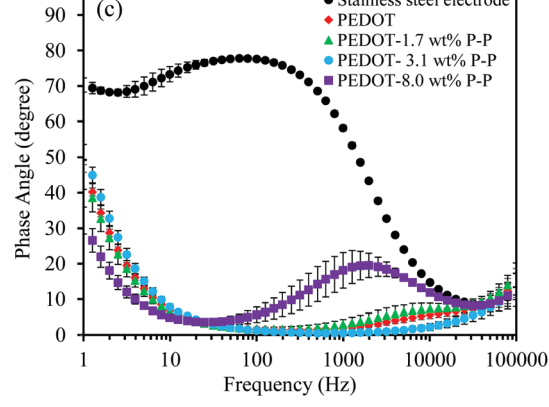


Fig. 3 Cyclic voltammetry (CV) and electrochemical impedance spectroscopy (EIS). (a) The CV curves of PEDOT and copolymer films were of similar shape while their charge storage capacities are significantly larger than that of stainless steel electrode. The oxidation peaks of these polymer films shifted to the positive direction with increasing amounts of crosslinker. These shifted oxidation peaks indicated that the crosslinker changed the conjugation length of PEDOT. (b) EIS of stainless steel, PEDOT and copolymer films deposited on stainless steel. The minor increase of impedance at high crosslinker concentration (8.0 wt%) indicated that crosslinker only has a slight effect on the impedance of the films. (Each point of EIS value was obtained by 3 measurements, and error bars show standard deviations). (c) Phase Angle of the EIS of stainless steel, PEDOT and copolymer films deposited on stainless steel. Stainless steel electrode is primarily functioning as a capacitor, and these polymer films are more like resistors.

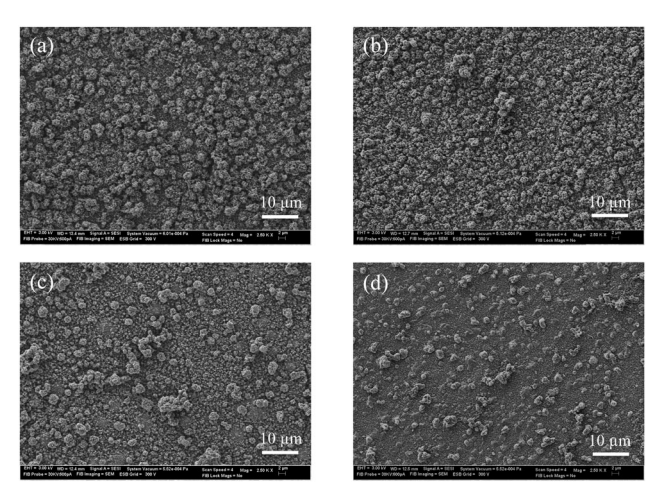
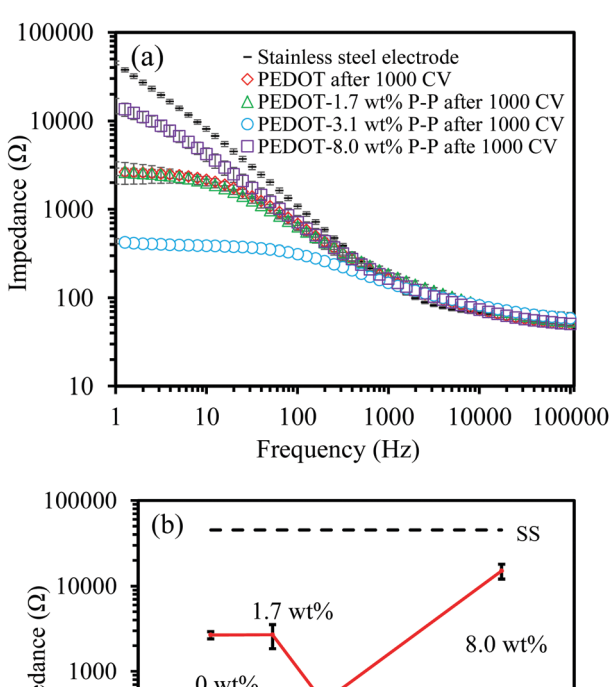


Fig. 4 SEM images of PEDOT and copolymer films. (a) PEDOT; (b) PEDOT-1.7 wt% P-P; (c) PEDOT-3.1 wt% P-P; (d) PEDOT-8.0 wt% P-P (scale bar represents $10~\mu m$).

concentration in the film and also had the highest impedance. The phase plot of the impedance spectroscopy revealed phase angles of $65\text{--}80^\circ$ for the bare stainless steel electrodes at frequencies of less than 1000 Hz which indicates that the electrode is primarily functioning as a capacitor (Fig. 3c). PEDOT coatings dramatically dropped the phase angles to a value below 20° making the electrodes more resistive as opposed to capacitive at frequencies above 5 Hz. There was a similar trend of the phase angle change for PEDOT and copolymers with low crosslinker concentration (<3.1 wt%) while it was different for the copolymer film with 8.0 wt% crosslinker indicating that there was also a structure change in the film.

3.5. Electrochemical stability

To determine their long-term electrochemical stability, the conjugated polymer coatings were studied by repeated CV tests in a PBS buffer solution at a scan rate of 100 mV $\ensuremath{\text{s}^{-1}}$ for 1000 consecutive cycles. After the CV cycling, the polymer films were subjected to EIS testing. Fig. 5 clearly shows that the copolymerization significantly affected the electrochemical stability of PEDOT films. With 1.7 wt% POSS-ProDOT in the feed, the copolymer film showed similar impedance spectra ($<3000 \Omega$) as the PEDOT film at the same deposition charge density. By increasing the POSS-ProDOT feed ratio to 3.1 wt%, a significant decrease in impedance magnitude ($\sim 400 \Omega$) was observed in comparison to the pure PEDOT film. When the POSS-ProDOT feed ratio was further increased to 8.0 wt%, the impedance benefit from the conjugated polymer coatings was again diminished. At 8.0 wt% POSS-ProDOT feed ratio, the impedance magnitude $(>10\,000~\Omega)$ of the coated electrode after the stability test was the same as the uncoated stainless steel electrode. The results are presumably due to the continuous swelling and shrinkage during the long-term charge/discharge process. The POSS-ProDOT crosslinks the PEDOT film, restricting the swelling and shrinkage of the polymer films during the oxidation and reduction process. For 1.7 wt% POSS-ProDOT feed ratio, only a few cross-linkers were incorporated into the polymer and thus the copolymer showed



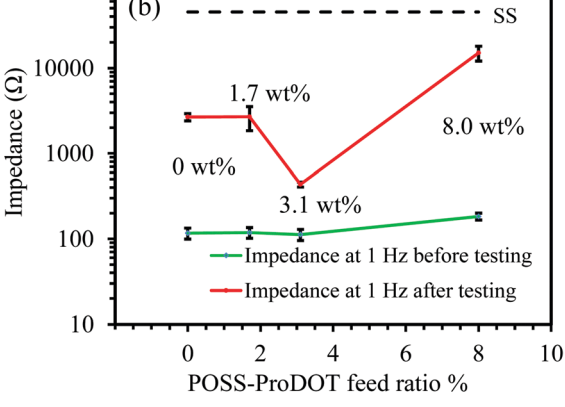


Fig. 5 Electrochemical impedance spectroscopy of PEDOT and copolymer films after stability test. (a) EIS after stability test showed that PEDOT with 3.1 wt% crosslinker performed the best. (b) Comparison of impedance at 1 Hz of PEDOT and copolymer films before and after stability test (each point of EIS value was obtained by 3 measurements, and error bars show standard deviations).

similar electrochemical stability as PEDOT. By increasing the feed ratio to 3.1 wt%, an intermediate amount of POSS-ProDOT was incorporated into the polymer and the strengthening effect helps to increase the stability of PEDOT coatings. At higher feed ratios (8.0 wt%) brittleness was observed, probably due to the high extent of intermolecular bonding from the excessive crosslinking within the polymer matrix. During the CV stimulations, ion exchange between the electrode and electrolyte lead to a certain amount of volumetric strain to the polymer coatings. This will lead to cracking and delamination if the associated strains are larger than the polymer coating's inherent strain to failure. The stability change of copolymer films was also confirmed by evaluating the morphology of the coatings after CV cycling by SEM. A comparison of the electrochemical impedance of stainless steel, PEDOT and copolymers at 1 Hz before and after stability tests is shown in Fig. 5b. The SEM images of the PEDOT and copolymer with various POSS-ProDOT contents are shown in Fig. 6. After the stability test, PEDOT film showed cracking and delamination which is consistent with literature. 20,21 By adding 1.7 wt% POSS-ProDOT, cracking was still observed but their sizes were much smaller. Films with 3.1 wt% POSS-ProDOT showed the most intact

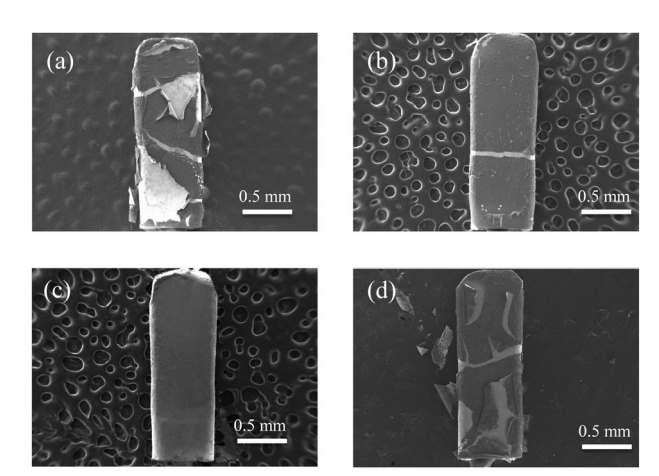


Fig. 6 Morphologies of PEDOT and copolymer films after stability test: (a) both cracking and delamination were observed on PEDOT film; (b) only cracking was found on PEDOT film with 1.7 wt% crosslinker; (c) no cracking nor delamination was found on PEDOT with 3.1 wt% crosslinker; (d) both cracking and delamination were observed on PEDOT film with 8.0 wt% crosslinker (scale bar represents 0.5 mm).

morphology with no obvious cracking or delamination. Polymer coatings with 8.0 wt% showed extensive cracking and delamination, similar to the pure PEDOT films. The trend of the effect of cross linker on the morphologies and electrochemical stability of PEDOT films correlated well with the EIS spectra.

4. Conclusions

In summary, we have synthesized an octa-ProDOT functionalized polyhedral oligomeric silsesquioxane (POSS-ProDOT) crosslinker via hydrosilylation and thiol-ene "click" chemistry. Its molecular structure was confirmed by both nuclear magnetic resonance (NMR) (1H, 13C, 29Si) and Fourier transform infrared (FT-IR) spectroscopies. The cross-linker was electrochemically copolymerized with EDOT in mixed monomer solutions to create cross-linked PEDOT:POSS-ProDOT copolymer films on metal electrodes. The optical, electrical and morphological properties of the copolymer films can be tuned by adjusting the feeding ratio of the cross linker. With more POSS-ProDOT incorporated into the films, the optical absorption shifted towards shorter wavelength direction, the impedance slightly increased and the morphology gradually changed from an open structure to a more closed structure. Significantly enhanced electrochemical stability was observed with the addition of POSS-ProDOT, with the optimum performance at 3.1 wt% POSS-ProDOT. Further additions of POSS-ProDOT led to the development of brittleness, as seen by cracking of the film. It is expected that these highly stable PEDOT-co-POSS-ProDOT materials will be excellent candidates for use in bioelectronic devices such as neural electrodes.

Acknowledgements

We thank the National Science Foundation (DMR-1103027, DMR-1505144), the National Institutes of Health through EUREKA grant 1RO1EB010892, the Defense Advanced Research Projects Agency (DARPA) grant N66001-11-C-4190, and the University of Delaware for funding. We thank Nandita Bhagwat for providing the ProDOT-ene monomer.

References

- 1 S. Cosnier, Anal. Bioanal. Chem., 2003, 377, 507.
- 2 Y.-Z. Long, M.-M. Li, C. Gu, M. Wan, J. Duvail, Z. Liu and Z. Fan, Prog. Polym. Sci., 2011, 36, 1415.
- 3 X. Luo, C. L. Weaver, D. D. Zhou, R. Greenberg and X. T. Cui, Biomaterials, 2011, 32, 5551.
- 4 S. J. Wilks, A. J. Woolley, L. Ouyang, D. C. Martin and K. J. Otto, Conf. Proc. IEEE Eng. Med. Biol. Soc., 2011, 5412.
- 5 E. Smela, Adv. Mater., 2003, 15, 481.
- 6 R. Balint, N. J. Cassidy and S. H. Cartmell, Acta Biomater., 2014, 10, 2341.
- 7 B. Zhu, S.-C. Luo, H. Zhao, H.-A. Lin, J. Sekine, A. Nakao, C. Chen, Y. Yamashita and H.-H. Yu, Nat. Commun., 2014,
- 8 H. Zhao, B. Zhu, J. Sekine, S.-C. Luo and H.-H. Yu, ACS Appl. Mater. Interfaces, 2012, 4, 680.
- 9 D. C. Martin, MRS Commun., 2015, 5, 131.
- 10 J. Liu, B. Wei, J. D. Sloppy, L. Ouyang, C. Ni and D. C. Martin, ACS Macro Lett., 2015, 4, 897.
- 11 R. A. Green, N. H. Lovell, G. G. Wallace and L. A. Poole-Warren, Biomaterials, 2008, 29, 3393.
- 12 L. Ouyang, C.-C. Kuo, B. Farrell, S. Pathak, B. Wei, J. Qu and D. C. Martin, J. Mater. Chem. B, 2015, 3, 5010.
- 13 R. A. Green and M. R. Abidian, Adv. Funct. Mater., 2015, 27, 7620.
- 14 B. Wei, J. Liu, L. Ouyang, C.-C. Kuo and D. C. Martin, ACS Appl. Mater. Interfaces, 2015, 7, 15388.
- 15 B. Wei, L. Ouyang, J. Liu and D. C. Martin, J. Mater. Chem. B, 2015, 3, 5028.
- 16 D. C. Martin, J. Wu, C. M. Shaw, Z. King, S. A. Spanninga, S. Richardson-Burns, J. Hendricks and J. Yang, Polym. Rev., 2010, 50, 340.
- 17 M. R. Abidian, K. A. Ludwig, T. C. Marzullo, D. C. Martin and D. R. Kipke, Adv. Mater., 2009, 21, 3764.
- 18 M. R. Abidian and D. C. Martin, Adv. Funct. Mater., 2009,
- 19 C. M. Frost, B. Wei, Z. Baghmanli, P. S. Cederna and M. G. Urbanchek, Plast. Reconstr. Surg., 2012, 129, 933.
- 20 T. A. Kung, N. B. Langhals, D. C. Martin, P. S. Cederna and M. G. Urbanchek, Plast. Reconstr. Surg., 2014, 133, 1380.
- 21 R. A. Green, R. T. Hassarati, L. Bouchinet, C. S. Lee, G. L. Cheong, J. F. Yu, C. W. Dodds, G. J. Suaning, L. A. Poole-Warren and N. H. Lovell, Biomaterials, 2012, 33, 5875.
- 22 S. Ghosh and O. Inganäs, J. Electrochem. Soc., 2000, 147, 1872.
- 23 S. Ghosh and O. Inganäs, Adv. Mater., 1999, 11, 1214.
- 24 D. Khodagholy, T. Doublet, M. Gurfinkel, P. Quilichini, E. Ismailova, P. Leleux, T. Herve, S. Sanaur, C. Bernard and G. G. Malliaras, Adv. Mater., 2011, 23, 268.

Paper

- 25 B. Wei, J. Liu, L. Ouyang, C.-C. Kuo and D. C. Martin, ACS Appl. Mater. Interfaces, 2015, 7, 15388.
- 26 S. Carli, L. Casarin, G. Bergamini, S. Caramori and C. A. Bignozzi, *J. Phys. Chem. C*, 2014, **118**, 16782.
- 27 I. Jerman, A. S. Vuk, M. Kozelj, B. Orel and J. Kovac, *Langmuir*, 2008, **24**, 5029.
- 28 J. Miyake, T. Sawamura, K. Kokado and Y. Chujo, *Macromol. Rapid Commun.*, 2009, **30**, 1559.
- 29 Y. Li, Q. Zhang, X. Zhao, P. Yu, L. Wu and D. Chen, *J. Mater. Chem.*, 2012, 22, 1884.
- 30 W. Wang, M. Chen, X. Chen and J. Wang, *Chem. Eng. J.*, 2014, 242, 62.
- 31 A. Luo, X. Jiang, H. Lin and J. Yin, *J. Mater. Chem.*, 2011, 21, 12753.
- 32 K. E. Feldman and D. C. Martin, Biosensors, 2012, 2, 305.

- 33 L. Groenendaal, G. Zotti, P.-H. Aubert, S. M. Waybright and J. R. Reynolds, Adv. Mater., 2003, 15, 855.
- 34 H.-B. Bu, G. Gotz, E. Reinold, A. Vogt, S. Schmid, R. Blanco, J. L. Segura and P. Bauerle, *Chem. Commun.*, 2008, 1320.
- 35 L. Qin, J. Xu, B. Lu, Y. Lu, X. Duan and G. Nie, *J. Mater. Chem.*, 2012, **22**, 18345.
- 36 M. Li, Y. Sheynin, A. Patra and M. Bendikov, *Chem. Mater.*, 2009, 21, 2482.
- 37 C. Lin, T. Endo, M. Takase, M. Iyoda and T. Nishinaga, *J. Am. Chem. Soc.*, 2011, **133**, 11339.
- 38 X. Cui and D. C. Martin, Sens. Actuators, B, 2003, 89, 92.
- 39 D. C. Martin and G. G. Malliaras, *ChemElectroChem*, 2016, 3, 686.
- 40 X. Cui and D. C. Martin, Sens. Actuators, A, 2003, 103, 384.